ISSN: 2476-6909; ECOPERSIA. 2020;8(2):97-107

An Improved Land Use Classification Scheme Using Multi-Seasonal Satellite Images and Secondary Data

ARTICLE INFO

Article Type
Original Research

Authors
Mirzaei S.[1] *MSc,*
Vafakhah M.*[2] *PhD,*
Pradhan B.[3] *PhD,*
Alavi S.j.[4] *PhD*

How to cite this article
Mirzaei S, Vafakhah M, Pradhan B, Alavi S.j. An Improved Land Use Classification Scheme Using Multi-Seasonal Satellite Images and Secondary Data. ECOPERSIA. 2020;8(2):97-107.

ABSTRACT

Aims Generally, optical satellite images are used to produce a land use map. Due to spectral mixing, these data can affect the accuracy of land use classifications, especially in areas with diverse vegetation.

Materials & Methods In the present study, in order to achieve the correct land use classification in a mountainous-forested basin, four Landsat 8 thermal images were used with a few additional information (Normalized Difference Vegetation Index (NDVI), Digital Elevation Model (DEM), slope angle and slope aspect) along with optical data and data of multi-temporal images.

Findings Results showed that thermal data, slope angle and DEM have a significant role in increasing the accuracy of land use classification, so that they increase the overall accuracy by about 3-10% from late spring to the beginning of autumn. Among the data used, slope angle and elevation data have a significant role in increasing the accuracy of agricultural classes. The total accuracy and Kappa coefficient in land use maps obtained from monotemporal images in the wet season (late spring; 83.93 and 0.82) and early summer (83.79 and 0.81)) are more than the dry season (late summer; 81.25 and 0.79) and early autumn).

Conclusion Generally, the highest total accuracy among monotemporal images generated from optical data is about 83.95%, while the application of thermal and additional data along with optical data and the combination of monotemporal images of the wet season, the accuracy of the information multitemporal increased to 91.60% of the land use map.

Keywords Land Use Classification; Remote Sensing; Landsat 8; Forested Area

[1]Watershed Management Engineering Department, Natural Resources Faculty, Tarbiat Modares University, Nur, Iran
[2]The Centre for Advanced Modelling & Geospatial Information Systems (CAMGIS), Engineering & Information Technology Faculty, University of Technology Sydney, Ultimo, Australia
[3]Energy & Mineral Resources Engineering Department, Sejong University, Seoul, South Korea
[4]Forestry Department, Natural Resources Faculty, Tarbiat Modares University, Nur, Iran

Correspondence
Address: Natural Resources Faculty, Tarbiat Modares University, Imam Khomeini Street, Imam Reza Boulevard, Nur, Mazandaran Province, Iran. Postal Code: 64414356
Phone: +98 (11) 44999120
Fax: +98 (11) 44553499
vafakhah@modares.ac.ir

Article History
Received: October 08, 2019
Accepted: December 07, 2019
ePublished: May 19, 2020

CITATION LINKS

[1] Assessment of remote sensing-based classification methods for ... [2] Investigation of quickbird satellite image capability in the separation of ... [3] Post-classification corrections in improving the classification of land use/land ... [4] Assessing land-use changes driven by river dynamics in chronically flood ... [5] Land use land cover change detection using remote sensing and GIS ... [6] Accuracy of land use change detection using support vector ... [7] Linking geomorphologic knowledge, RS and GIS ... [8] Improving the accuracy of land use and land cover classification of landsat ... [9] Application of support vector machines for landuse ... [10] Improving classification accuracy of multi-temporal ... [11] Longterm land use change detection in Mahidasht watershed ... [12] Land management and land-cover change have impacts of similar magnitude on ... [13] Comparison of accuracy measures for RS image classification using SVM and ... [14] Mapping land cover in complex Mediterranean ... [15] Multi-temporal land use classification using hybrid ... [16] Improved crop classification using multitemporal RapidEye ... [17] Parcel-level identification of crop types using different ... [18] Land cover mapping based on random forest classification ... [19] Towards improved land use mapping of irrigated ... [20] Incorporating ancillary data into landsat 8 image ... [21] Land use change prediction using a hybrid ... [22] Assessing the potential of integrated landsat ... [23] Improved land-use/land-cover classification ... [24] The improvement of land cover classification ... [25] Assessment of multi-temporal, multi-sensor radar and ... [26] A semi-supervised hybrid approach for multitemporal multi-region ... [27] Modeling land use changes of Ramin city in the Golestan ... [28] The global landsat archive: Status, consolidation ... [29] A survey of image classification methods ... [30] Comparison of supervised classification methods on ... [31] Controls on peak discharge at the lower course ... [32] Land cover classification using landsat 8 operational ... [33] land-use and land-cover classification in semi-arid regions ... [34] Fundamentals of satellite remote ... [35] Multi-temporal landsat images and ancillary data for land ... [36] The function and metabolism of ascorbic ... [37] SRTM-DEM and landsat ETM+ data for mapping tropical dry forest ...

Introduction

Land use classification with satellite images is widely used in remote sensing data processing by which meaningful thematic maps are produced from satellite images [1], and the combination of remote sensing (RS) and geographic information system (GIS). Due to increasing improvements in remote sensing and geographic information system, exploiting these methods can be considered as a suitable option to provide spatial and descriptive information [2] and application provides a powerful and cost-effective approach for land-use mapping [2-5]. The up-to-date and reliable information from the land use map and their land cover dynamics provides key information to the managers, which help in adopting proper managerial decisions in watershed management [3]. However, achieving reasonable results is not easy due to the data limitation, data type, pre-processing of satellite images, classification methods and land use complexities and land cover types [6-8]. Different methods of classification are presented over the past three decades, many studies have been conducted to verify the accuracy of classification methods, and as a result, new and improved classification algorithms were developed. For example, over recent decades, Maximum Likelihood Classifier (MLC) and Artificial Neural Network (ANN) have been popularly used, and among new algorithms, Support Vector Machines (SVM) [9] is commonly applied.

Similar spectral properties of the type of land cover make the classification process more complicated. This is very evident in agricultural applications, especially when mono-temporal satellite imagery is used [10]. For example, heterogeneous regions due to the presence of small pieces of several land use, dispersal of urban areas, high reflection of very dry soils and areas with limestone which affects vegetarian cover and ultimately in areas where mixed dry farming exists, the utilization of one image may make the land-use analysis difficult [11].

The application of mono-temporal optical remote sensing data has been widely used in many studies because of accelerating the individual image processing [2, 3, 6, 9, 12-14].

In order to overcome such difficulties, various strategies should be used in land use classification. In some studies, for example, multi-temporal images [13-16], and in some other studies, a combination of secondary data such as physiographic factors (elevation, slope, and soil type) and vegetation indices (NDVI and NDWI) [2, 17, 18], and in other researches, a combination of secondary data and multi-temporal images [10, 19, 20], are employed. Accordingly, many researchers have increased the accuracy of land use classification using satellite imagery [10, 21-25].

Using these strategies, the obtained accuracy increases compared with land use and land cover maps generated from the optical data of the mono-temporal images. The major challenge in land use classification using mono-temporal multidimensional data is that uncertainty arises from the differences of changes in different factors over time, such as different phenological periods or mixed vegetation changes, different shapes and textures [18]. Therefore, the spectral data of a point at a given time of satellite images cannot provide comprehensive information about the phenological period of vegetation and the temporal characteristics of each land use [16]. Hence, a land use classification at an inappropriate time will be accompanied by more plural [26]. Since the multi-temporal satellite imagery provides spectral information of various phenological stages of vegetation, so the use of multi-time images allows for the separation of different vegetation coverage with similar spectral properties [17]. In fact, changes due to different seasons' vegetation coverage are included in multi-temporal land use classification, which can be very helpful in understanding the land use dynamics in natural resources [16]. Thus, besides its application for increasing the agricultural products' and other plant species' classification accuracy, it is suitable to use multi-temporal data for separating agricultural vegetation from natural vegetation coverage [11] and have an important role in resources management and helps managers to better planning of land use [27].

Several studies have been conducted applying different strategies to enhance accuracy of land use maps, however, there is no available study on using several strategies at once as an integrated approach to enhance accuracy of land use maps. Therefore, the present study aimed to apply the most commonly used strategies together and investigate their effect on the enhancement of land use maps' accuracy

individually and together. The strategies are described as follows:

1- Mono-temporal classification by optical data

2- Mono-temporal classification by optical and thermal data

3- Mono-temporal classification by optical data, thermal and secondary data (NDVI, DEM, slope and slope aspect)

4- Multi-temporal classification by optical data

5- Multi-temporal classification by optical, thermal and secondary data (NDVI, DEM, slope and slope aspect)

Study area

The Talar Watershed with an area of 1,765km^2 is located in northern Iran at the geographical location of 52°35′44" to 53°23′19" eastern longitude and 35°44′7" to 36°18′20" northern latitude. The Talar Watershed is drained by a river called "Talar" which is shown in Figure 1. The average elevation of the watershed is 1978m above sea level, and the average slope is 40%. Wet air flow inclination in heights due to the fact that the watershed is located adjacent to the Caspian Sea, causing orographic precipitation.

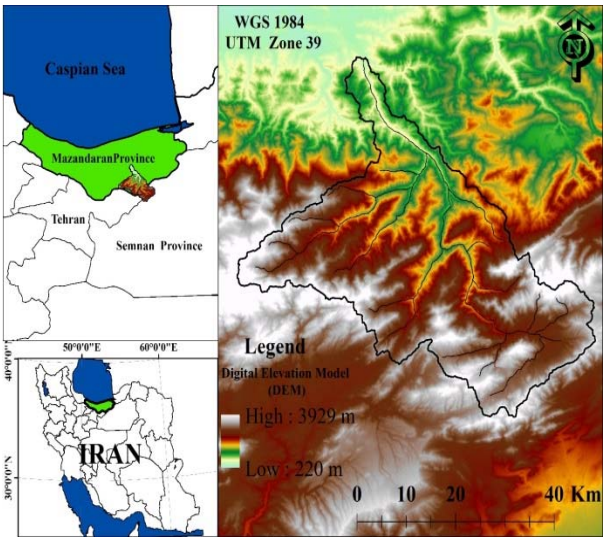

Figure 1) Location of the Talar Watershed in the north of Iran

Materials and Methods

Satellite data

Landsat series images are a reliable source for examining land cover variations due to the 30 meter spatial resolution and the 185 swath and the 16-day imaging cycle [15]. On the other hand, access to high-resolution satellite data is mostly limited due to their high cost. Hence because of the free access to the Landsat image archive, these data are one of the best available satellite data that can provide significant solutions for land cover mapping [28]. In the present study, the TIRS-OLI Landsat multi-temporal images of Landsat 8 in non-cloudy conditions [19] were obtained from USGS in 2017. Besides spectral of 1 to 7 (1: Aerosol/coastal; 2: Blue; 3: Green; 4: Red; 5: Near-infrared; 6 and 7: Short wave infrared), as well as thermal 10 (TIR1: Thermal infrared) for land use classification were used (Table 1).

Table 1) Specifications of Landsat 8 satellite images used in the study

Row	Path	Date	Sensor
35	163	31 May 2017	OLI-IRS
35	163	2 Jul 2017	
35	163	20 Sep 2017	
35	163	22 Oct 2017	

Image Pre-processing

Radiometric correction is necessary to calculate the Normalized Difference Vegetation Index (NDVI) [18, 26]. Therefore, for radiometric correction, the DN values of the image were calibrated to radiation [2, 19], then the atmospheric correction was performed using the FLAASH module [14, 19, 21, 27].

Ancillary data

Land use is influenced by various parameters, so that the spectral information along with the characteristics data of the Earth such as elevation, slope, and slope aspect considerably increases the accuracy of the land use classification [10, 17, 19, 28]. This information, especially in mountainous regions, where vegetation distribution is closely related to topography, plays an important role in increasing the accuracy of vegetation cover classification [29]. The Talar Watershed is a mountainous area where irrigated agricultural lands are largely spread along the rivers, especially the main river, with lands of lower elevations and slopes. In the study area, forest cover can be often seen up to 2500m a.s.l. level, and at higher altitudes, due to reduced rainfall, rangeland cover is a substitute for forest cover. Therefore, in the present study, using ASTER derived DEM (30m), slope aspect and slope information is extracted, and using spectral information of red and infrared bands NDVI. The brightness temperature was considered as ancillary information factors for land use classification (Figure 2).

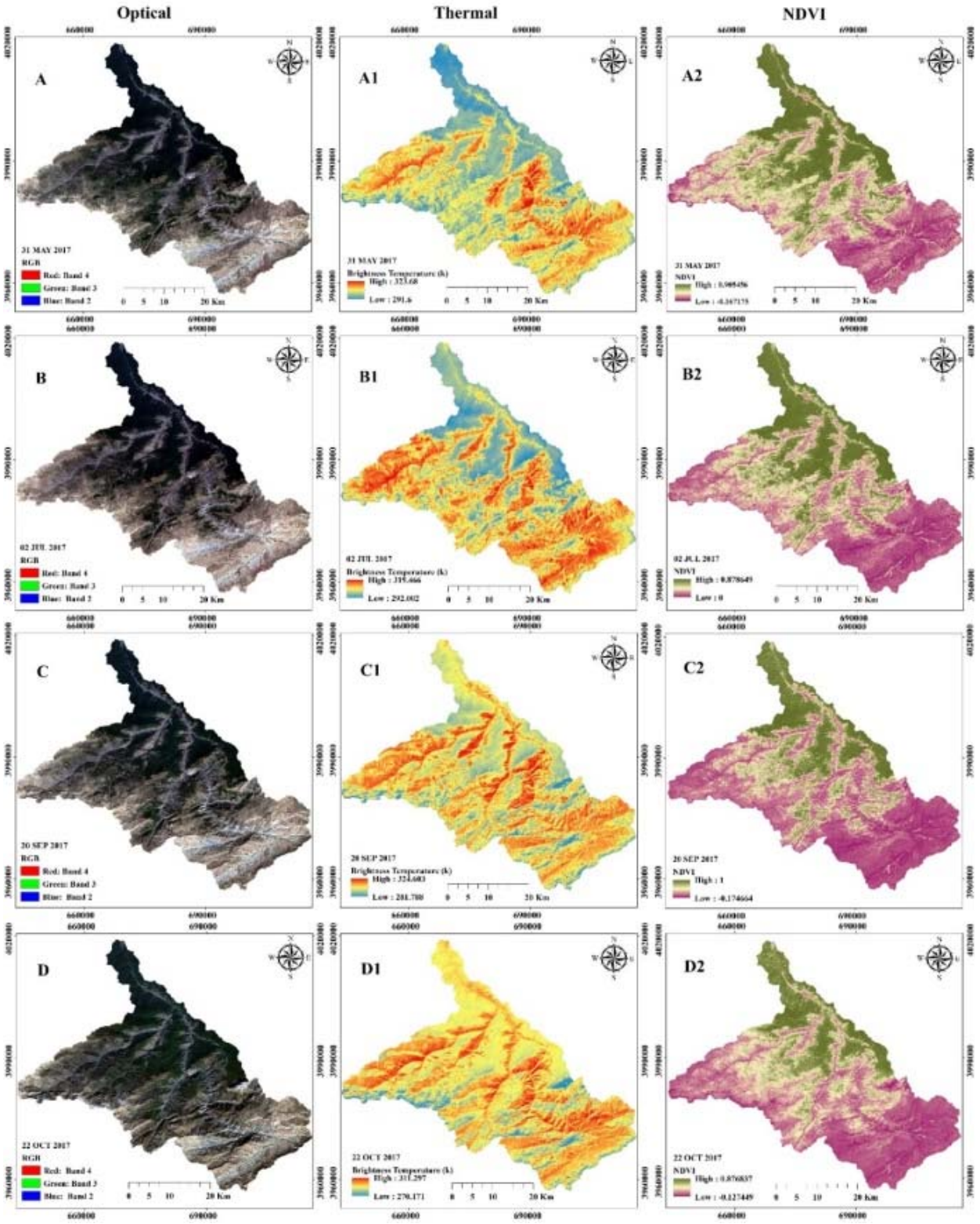

Figure 2) Optical bands with a natural color combination (A, B, C, and D), brightness temperature obtained from the thermal bond (A1, B1, C1, and D1), NDNI index (A2, B2, C2, and D2)

Classification

Maximum Likelihood Classification (MLC) algorithm is one of the most popular supervised classification algorithms widely used for land use/land cover (LULC) mapping [13, 16, 19, 30]. The MCL algorithm examines the covariance and variance of spectral response patterns of a group when classifying an unknown pixel. Thus, it is assumed that the distribution of cloudpoints that comprise the training data of that group is Gaussian, i.e. a normal distribution [30].

Based on this assumption, the distribution behavior of each group with the spectral response pattern can be described with the mean vector and covariance matrix. Therefore, each pixel is classified into a class with the highest likelihood, which can be categorized as an index of certainty, while the classification of pixels with the maximum likelihood below the threshold is rejected [31]. Regarding the spectral properties of images and recognition of land use in the studied area [3], eight land use categories including residential land (RL), Arid Land (BL), Dryland agriculture (DF), irrigated agriculture (IF), poor range (R3), medium range (R2), medium forests (F2), and good forests (F1) were considered.

Multi-temporal method

The LULC map derived from the MLC algorithm in single-stroke images due to the similarity of the spectral reflection of the various classes has errors in which the pixels of some uses have similar spectral reflections that interfere with forest, agricultural land and range and are categorized incorrectly [2, 14]. This misclassification is related to the phenological period of the vegetation, and the accuracy of the map is different in different seasons and months of a year [19, 21]. The watershed has diverse LULC, but the time share of the phenological period of plants of different land use in some seasons of the year, such as the late spring, reflects the spectrum of rangeland, agriculture and forest cover, which has a more spectral mix.

So, using single-shot image classification, there is no access to the most accurate use classes. For this reason, combining multi-temporal image information can be useful in increasing the accuracy of the classifications. For this purpose, in the present study, the first four classes of images were classified as late spring, early summer, late summer, and early fall with or without ancillary information. Then, from the four land use maps produced, two maps with the highest accuracy were used to combine the information as well as the preparation of a multi-temporal land use map.

Accuracy assessment

One of the most common methods for evaluating classification accuracy is through the confusion matrix. Accordingly, 511 ground truth samples were made using GPS. To compare the results of classification and ground truth, the producer accuracy criteria, user accuracy, overall accuracy, and Kappa coefficient obtained from the confusion matrix were used [32]. The producer accuracy is to measure the correct classification and the probability of a pixel being classified in the same class, while the user accuracy is the measure of the reliability of the map for each class and the probability that a given class on the ground will be located in the same class in the classified image [33]. The overall accuracy is the correct percentage of classified pixels, and the Kappa coefficient is an accuracy measurement method that evaluates the degree of agreement compared to the random classification [34] and represents the overall accuracy agreement with the real state of nature [14]. Figure 3 presents the general flowchart of the research steps.

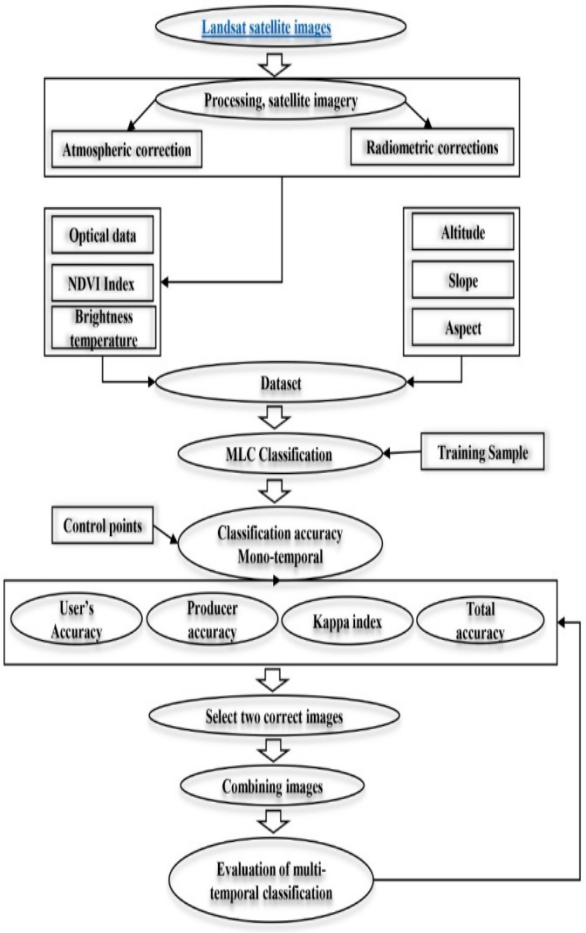

Figure 3) Flowchart of research methodology

Findings

Evaluation of single-shot classification

The results of the classification of images with optical data showed that the classification accuracy decreases from late spring to early fall

(Table 2), so that the image of 31st May 2017 with a total accuracy of 83.95 and a Kappa coefficient of 0.8158 had the highest classification accuracy among the most related images and the images of 22nd October 2017 with a total accuracy of 74.22 and a Kappa coefficient of 0.7042 had the lowest classification accuracy.

The results of the classification of images with optical data showed that the classification accuracy decreases from late spring to early fall. By adding the brightness temperature data to the total optical data of the images and land use classification, the overall accuracy and Kappa index increased in images except for the late spring. As the overall classification accuracy of images of July 2nd, September 20th, and October 22nd with optical and thermal information relative to the classification of optical data is increased (Table 3). The NDVI index, with the exception of the late spring (31st May), on other dates, has reduced classification accuracy. By adding DEM to the total optical and thermal data in all images (late spring to early fall), the accuracy of the classification increases. The slope information after thermal information has a significant role in increasing the accuracy of classification in all images, as the overall accuracy in the early spring and late summer increased by about 2.5%. In total, with the addition of ancillary information to the optical data, the total accuracy increased (Figure 4).

Evaluation of multi-temporal classification accuracy

Land use maps of the aforementioned dates were merged and areas that had different land uses in the two maps were decided in terms of more appropriate class by examining them in Google Earth. Investigation of the variation matrix of land use map of the mentioned dates obtained from the optical data indicated that the maximum change area (4.43km^2) relates to the areas in the 31st May map related to poor rangeland (R3) and in 2nd July map it was categorized as DF (Table 4). Investigating the relevant areas in Google Earth showed that these areas are mostly farmed with as DF, so the final class of these areas is DF. After these areas, areas with an area of 35km^2 on 2nd July were categorized as R3, and on the 31st May were categorized as IF. Examining these areas with Google Earth showed that these areas are mostly R3. Areas with an area of 30km^2 mapped on 31st May and 2nd July were classified as DF and R3, respectively.

The land use change matrix of the aforementioned dates, using the total optical, thermal and additional information showed that the most significant changes with an area of 48km^2 were those of the areas described in the 31st May map BL and in the 2nd July map is classified as R3 (Table 5). Examining these areas in Google Earth shows that the correct use of these areas is R3. After these areas, an area of 45km^2 mapped on 31st May was classified as R2 and on the 2nd July map as the medium forest class. Checking the accuracy of these areas with Google Earth shows that these areas are mainly in R2 class. The area of 29km^2 in map of 31st May was classified as R3 class and in the 2nd July map it was classified as BL, which using Google Earth the R3 was considered to be a more correct class (Figure 5).

Table 2) Evaluation of land use accuracy by adding parameters to optical data (O: Optical; T: Thermal; N: NDVI; D: DEM; S: Slop; A: Slope aspect)

Dataset	O	O and T	O, T and N	O, T and D	O, T, D and S	O, T, D, S and A
05/31/2017						
Overall Accuracy	83.95	83.79	84.38	85.49	87.89	87.50
Kappa	0.8158	0.8143	0.82	0.83	0.86	0.85
07/02/2017						
Overall Accuracy	83.79	86.33	85.74	87.70	89.65	89.45
Kappa	0.81	0.84	0.83	0.85	0.88	0.87
09/20/2017						
Overall Accuracy	81.25	84.77	83.79	85.16	87.70	87.89
Kappa	0.78	0.82	0.81	0.82	0.85	0.86
10/22/2017						
Overall Accuracy	74.22	79.10	77.93	81.25	83.01	83.79
Kappa	0.70	0.76	0.74	0.78	0.80	0.81

Table 3) Rate of increase in overall accuracy and Kappa by adding parameters (O: Optical; T: Thermal; N: NDVI; S: Slop; A: Slope aspect)

Dataset	O and T	O, T and N	O, T and D	O, T, D and S	O, T, D, S and A
05/31/2017					
Overall Accuracy	-0.16	0.59	1.7	2.4	-0.39
Kappa	-0.001	0.006	0.024	0.022	-0.004
07/02/2017					
Overall Accuracy	2.54	-0.59	1.37	1.95	-0.2
Kappa	0.029	-0.006	0.015	0.022	-0.002
09/20/2017					
Overall Accuracy	3.52	-0.98	0.39	2.54	0.19
Kappa	0.040	-0.011	0.004	0.029	0.002
10/22/2017					
Overall Accuracy	4.88	-1.17	2.15	1.76	0.78
Kappa	0.056	-0.013	0.024	0.020	0.008

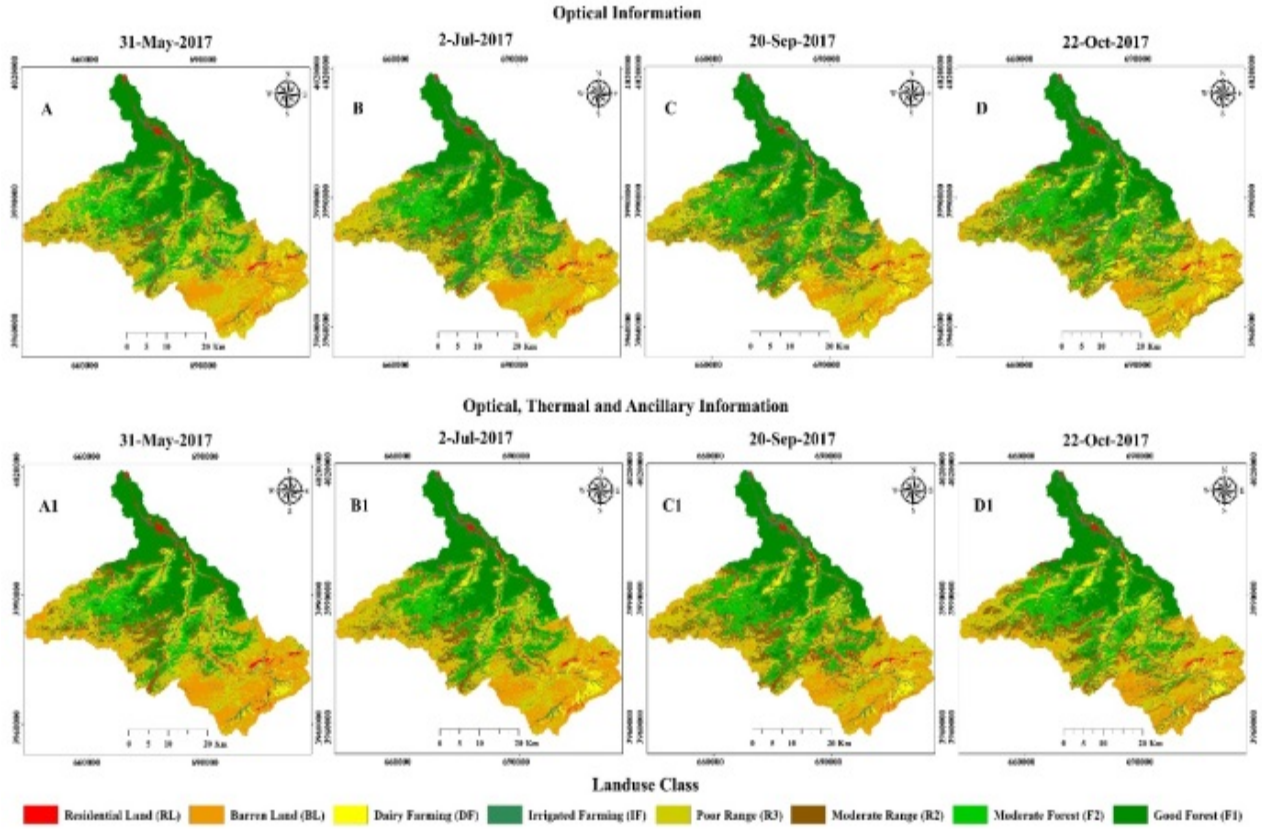

Figure 4) Single-shot land use map with optical data (A, B, C, and D) and total optical, thermal and additional data (A1, B1, C1, and D1)

Table 4) Land use change matrix (31st May; column and 2nd July; row) using optical information (km²)

		31-May-2017									
	LU/LC Classes	**RL**	**BL**	**DF**	**IF**	**R3**	**R2**	**F2**	**F1**	**Row Total**	**Class Total**
2-July-2017	**RL**	24.86	3.11	2.36	5.01	1.33	0.6	0.46	0	37.73	37.75
	BL	1.11	2941.39	6.88	10.19	20.05	0.13	0.03	0	2979.77	2979.95
	DF	1.85	13.67	39.24	5.19	43.59	5.88	0.38	0	109.81	109.83
	IF	6.16	6.7	20.44	82.95	34.83	19.78	12.65	5.2	188.7	188.97
	R3	0.92	28.41	30.25	15.06	312.83	7.45	0.29	0	395.21	395.37
	R2	0.55	0.01	22.89	8.85	16.61	84.3	16.35	0.03	149.59	149.59
	F2	0.12	0.17	6.78	10.36	6.03	22.97	190.08	3.49	240	240
	F1	0.04	0	0.14	5.46	0	1.2	5.79	376.9	389.52	389.52
	Class Total	35.62	2993.45	128.97	143.05	435.27	142.32	226.02	385.62		
	Class Changes	10.76	52.07	89.73	60.11	122.44	58.01	35.95	8.72		
	Image Difference	2.13	-13.5	-19.15	45.92	-39.9	7.27	13.97	3.9		

Table 5) Land use change matrix date 31st May (column) and 2nd July (row) using total optical, thermal, and additional information (per km²)

2-July-2017 \ 31-May-2017	RL	BL	DF	IF	R3	R2	F2	F1	Row Total	Class Total
RL	27.7	2.82	3.73	4.02	5.01	2.98	1.58	0.16	47.99	48.08
BL	1.98	248.29	0.84	2.39	29.05	0.05	0.13	0	282.75	282.98
DF	3.63	8.24	39.79	5.61	22.37	4.02	1.68	0	85.34	85.34
IF	4.91	2.43	5.45	36.45	5.42	10.86	1.79	3.57	70.88	70.9
R3	4.93	48.1	16.08	9.97	356.02	13.77	6.37	0	455.24	455.43
R2	1.54	0.11	13.42	3.12	21.61	105.44	27.95	0.34	173.53	173.56
F2	1.37	0.03	5.12	2.68	3.74	44.94	191.62	5.48	254.97	254.98
F1	0.76	0	0.32	1.19	0	5.21	10.1	373.45	391.03	391.03
Class Total	46.82	310.01	84.75	65.44	443.22	187.28	241.22	382.99		
Class Changes	19.13	61.72	44.96	28.99	87.2	81.83	49.6	9.55		
Image Difference	1.26	-27.03	0.58	5.46	12.21	-13.72	13.76	8.04		

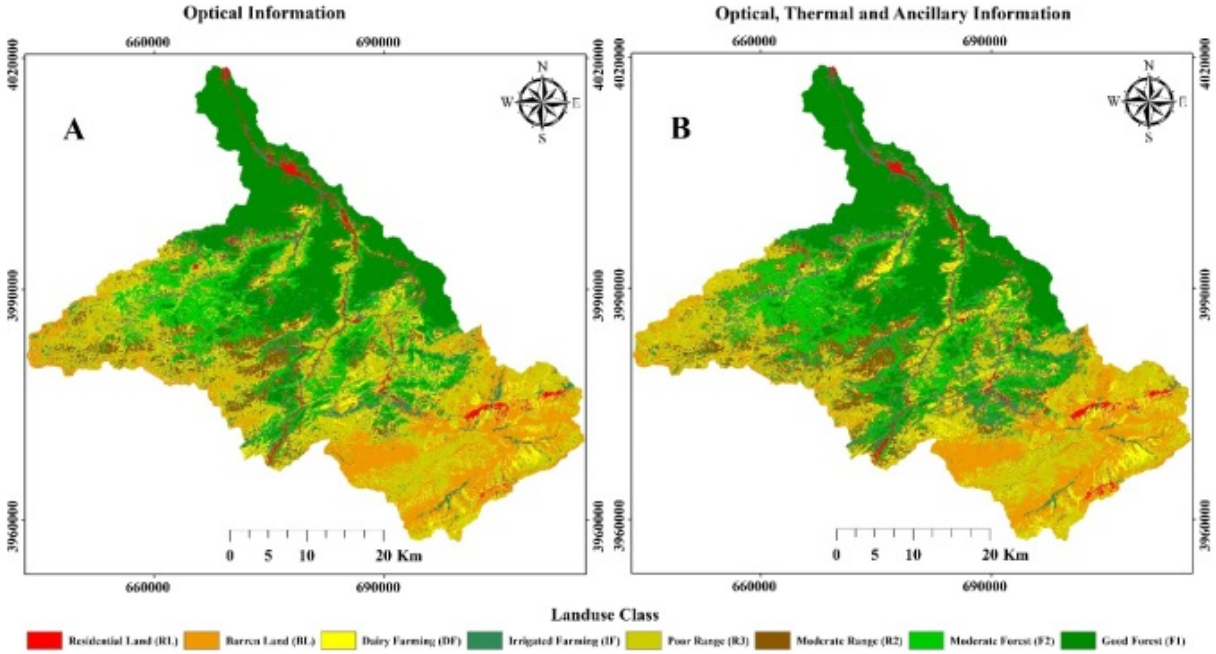

Figure 5) Multi-temporal map using optical information (A) as well as total of optical, thermal and ancillary information (B)

Table 6) Producer and user accuracies multi-temporal land use map produced by optical data alone and using total optical, thermal and data

Data set	Optical		Optical, Thermal and Ancillary Data	
LU/LC Classes	Prod. Acc	Use. Acc	Prod. Acc	Use. Acc
Residential Land (RL)	78.85	93.18	94.23	92.45
Barren Land (BL)	71.79	66.67	88.31	89.47
Dairy Farming (DF)	100	100	86.21	87.72
Irrigated Farming (IF)	88.89	91.14	97.44	79.17
Poor Range (R3)	80.28	79.17	100	100
Moderate Range (R2)	89.66	66.67	83.1	88.06
Moderate Forest (F2)	66.23	82.26	90.12	94.81
Good Forest (F1)	100	98.55	97.06	97.06
Overall Accuracy	84.96		91.60	
Kappa	0.8274		0.9036	

The evaluation of the accuracy of the multi-temporal land use map showed that in both multi-temporal land use maps (based on optical data and total optical, thermal and additional data), the overall accuracy and Kappa coefficient increased (Table 6), so that the

overall accuracy and Kappa coefficient of the map generated from optical data on 31st May and 2nd July increased from 83.95, 0.8158 and 83.79, 0.8140 to 84.96, 0.8274, respectively. In other words, the accuracy of multi-temporal mapping compared to single-shot has increased by about 1% using optical data. The overall accuracy and Kappa coefficient of the generated map by optical, thermal and additional data on May 31st and July 2nd increased from 87.89, 0.8610 and 89.65, 0.8812 to 91.60, 0.9036. It means that the accuracy of the multi-temporal land-use map has increased by about 2% using optical, thermal and additional data.

Discussion

The results showed that the overall accuracy and Kappa coefficient of the land use data obtained from Landsat 8 optical data varies from 83.95% and 0.8151 in late spring to 74.22% and 0.7042 in late fall, respectively (Table 2). This finding shows that the accuracy of the map produced in the wet season is more accurate than the dry season, which is similar to the findings of Kantakumar and Neelamsetti and Zoungrana *et al*. [16, 35]. The accuracy of separation F1, F2, and RL is the highest in all four images. The distinctive features and spectral resolution of the forest class are narrowly segregated due to less spectral mixing, while the separation of agricultural and rangelands classes is less accurate due to the spectral similarity of these classes increases the probability of spectral mixing and thus increases the misclassification [3]. With the addition of thermal data (thermal infrared band: TRS1) to optical data and land use classification, the overall accuracy and Kappa coefficient are slightly reduced in the map of the early spring image, but from early summer to early fall it increased so that in the early summer, overall accuracy and Kappa coefficient increased by 2.54% and 0.0292, respectively, and by early fall, it increased by 4.88% and 0.056, respectively (Table 3) This is related to the difference in brightness temperature of the of land use in different seasons (Figure 4), so that from late spring to early fall, the difference in brightness temperature increases, so in early fall, the difference in brightness is greater in land use, and facilitates the classification. Increasing the land use accuracy by combining optical and thermal information has been reported in several studies [9, 25, 33, 35]. In fact, the use of thermal data along with other spectral bands to produce a land use map facilitates the classification with similar spectral properties or similar phenologies [10]. On the other hand, with the addition of thermal information, the accuracy of classification of BL and DF has increased more than others.

Several studies have reported that the use of additional information such as elevation, slope and vegetation indices will increase the classification accuracy [17, 18, 34]. In the current study, with the addition of the NDVI index to the optical and thermal data, only in the late spring image, the overall accuracy and Kappa coefficient increase slightly, but in the other images, the accuracy is slightly reduced (Table 3). This is due to the fact that in late spring, the R3, due to its phenological timing, still has chlorophyll content, and therefore, by adding NDVI it provides a complete set of optical and thermal information, user and producer accuracy of this land use increases significantly, but with the arrival of the summer season, the vegetation is dry or decreasing. As a result, in images of early summer to early fall, the increase in the accuracy increased slightly by adding NDVI index. On the other hand, rain-fed farming lands dry in summer, then adding DEM data leads to interfacing of uncovered uses (rain-fed cover and dry land) and thus reduces the accuracy of the land use mapping. By adding DEM to the optical and thermal data, the accuracy of land use classification increases significantly, so that the overall accuracy rises from about 1% in late spring to about 4% in early fall (Table 3). Sesnie *et al*. [36], in a study in Nicaragua's tropical forest used a DEM also reported an increase in the accuracy of the entire land use classification by about 5%. Among the land use classes, the use of DEM significantly increased the user and producer accuracy of agricultural classes.

Among the single-shot maps produced by optical data (Figures 4-A, 4-B, 4-C, and 4-D), images of the late spring and early summer were respectively with overall accuracy and Kappa coefficient of 83.95%, 0.8158 and 83.79%, 0.8140 had the highest accuracy (Table 3). By adding thermal data and additional information (NDVI, DEM, slope and slope aspect) to optical data (Figures 4-A1, 4-B1, 4-C1, and 4-D1), the overall accuracy and Kappa coefficient in the same images increased to 87.89, 0.8610, and 89.45, 87.90 (Table 3) which

were the highest overall accuracy and Kappa coefficient among other land user maps.

Conclusion

In the present study, the application of thermal data and additional information (NDVI, DEM, slope angle, and slope aspect) along with optical data as well as multi-temporal images to increase the accuracy and improve the accuracy of land use classification was investigated. The results showed that thermal data, slope and elevation had a significant role in increasing the accuracy of land use classification, increasing the overall accuracy by about 3-10% from late spring to early fall. Given the mountainousness nature of the area, slope and elevation information increased the accuracy of agricultural classes, since agricultural development is limited to climatic conditions and the possibility of agricultural operations, which are related to topography (elevation and slope). Among the user maps derived from single-shot images, the total accuracy and Kappa coefficient in the wet season (late spring and early summer) were higher than the dry season (late summer and early spring). The results of the integration of wet season maps indicated that the map obtained from the integration of optical data as well as the total optical data, thermal data and additional information (NDVI, DEM, slope and slope aspect) increases slope the overall accuracy of the classification by about 2%. Generally, the highest accuracy of the maps produced using optical data was with 83.95% was related to at the late spring, while using all strategies for increasing the accuracy of classification, the highest overall accuracy (95.61) was related to multi-temporal images of wet season.

Acknowledgments: The authors are profoundly grateful to two anonymous reviewers for their appropriate and constructive suggestions.

Ethical Permission: The case was not found by the authors.

Authors Contribution: Sajjad Mirzaei (First author), Introduction author/Original researcher/Statistical analyst (45%); Mehdi Vafakhah (Second author), Introduction author/Methodologist/Discussion author (30%); Biswajeet Pradhan (Third author), Introduction author/Discussion author (15%); Seyed Jalil Alavi (Fourth author), Introduction author (10%)

Conflicts of Interests: The authors declare that there is no conflict of interests regarding the publication of this study.

Funding/Supports: The current study was supported by Tarbiat Modares University.

References

1- Afrasinei GM, Melis MT, Buttau C, Bradd JM, Arras C, Ghiglieri G. Assessment of remote sensing-based classification methods for change detection of salt-affected areas (Biskra area, Algeria). J Appl Remote Sens. 2017;11(1):016025.

2- Naseri MH, MotazedianM. Investigation of quickbird satellite image capability in the separation of the canopy of Zagros forest trees. Ecopersia. 2019;7(3):149-54.

3- Thakkar AK, Desai VR, Patel A, Potdar MB. Post-classification corrections in improving the classification of land use/land Cover of arid region using RS and GIS: The case of Arjuni watershed, Gujarat, India. Egypt J Remote Sens. 2017;20(1):79-89.

4- Hazarika N, Das AK, Borah SB. Assessing land-use changes driven by river dynamics in chronically flood affected Upper Brahmaputra plains, India, using RS-GIS techniques. Egypt J Remote Sens Sp Sci. 2015;18(1):107-18.

5- Phukan P, Thakuriah G, Saikia R. Land use land cover change detection using remote sensing and GIS techniques: A case study of Golaghat district of Assam, India. Int Res J Earth Sci. 2013;1(1):11-5.

6- Karan SK, Samadder SR. Accuracy of land use change detection using support vector machine and maximum likelihood techniques for open-cast coal mining areas. Environ Monit Assess. 2016;188(8):486.

7- López-Granados E, Mendoza ME, González DI. Linking geomorphologic knowledge, RS and GIS techniques for analyzing land cover and land use change: A multitemporal study in the Cointzio watershed, Mexico. Rev Ambient Água. 2013;8(1):18-37.

8- Manandhar R, Odeh IO, Ancev T. Improving the accuracy of land use and land cover classification of landsat data using post-classificatio
n enhancement. Remote Sens. 2009;1(3):330-44.

9- Ustuner M, Sanli FB, Dixon B. Application of support vector machines for landuse classification using high-resolution rapideye images: A sensitivity analysis. Eur J Remote Sens. 2015;48(1):403-22.

10- Gomariz-Castillo F, Alonso-Sarría F, Cánovas-García F. Improving classification accuracy of multi-temporal Landsat Images by Assessing the Use of different algorithms, textural and ancillary information for a mediterranean semiarid area from 2000 to 2015. Remote Sens. 2017;9(10):1058.

11- Gheitury M, Heshmati M, Ahmadi M. Longterm land use change detection in Mahidasht watershed, Iran. Ecopersia. 2019;7(3):141-8.

12- Luyssaert S, Jammet M, Stoy PC, Estel S, Pongratz J, Ceschia E, et al. Land management and land-cover change have impacts of similar magnitude on surface temperature. Nat Clim Change. 2014;4(5):389-93.

13- Prasad SV, Savithri TS, Krishna IV. Comparison of accuracy measures for RS image classification using SVM and ANN classifiers. Int J Electr Comput Eng. 2017;7(3): 1180-7.

14- Senf C, Leitão PJ, Pflugmacher D, Van Der Linden S, Hostert P. Mapping land cover in complex Mediterranean landscapes using landsat: Improved classification accuracies from integrating multi-seasonal and synthetic imagery. Remote Sens Environ. 2015;156:527-536.

15- Kantakumar LN, Neelamsetti P. Multi-temporal land use classification using hybrid approach. Egypt J Remote Sens Sp Sci. 2015;18(2):289-95.
16- Beyer F, Jarmer T, Siegmann B, Fischer P. Improved crop classification using multitemporal RapidEye data. 8th International Workshop on the Analysis of Multitemporal Remote Sensing Images (Multi-Temp), 2015 July 22-24, Annecy, France. Piscataway: IEEE; 2015.
17- Alganci U, Sertel E, Ozdogan M, Ormeci C. Parcel-level identification of crop types using different classification algorithms and multi-resolution imagery in Southeastern Turkey. Photogramm Eng Remote Sens. 2013;79(11):1053-65.
18- Eisavi V, Homayouni S, Yazdi AM, Alimohammadi A. Land cover mapping based on random forest classification of multitemporal spectral and thermal images. Environ Monit Assess. 2015;187(5):291.
19- Basukala AK, Oldenburg C, Schellberg J, Sultanov M, Dubovyk O. Towards improved land use mapping of irrigated croplands: Performance assessment of different image classification algorithms and approaches. Eur J Remote Sens. 2017;50(1):187-201.
20- Nguyen TT, Pham TT. Incorporating ancillary data into landsat 8 image classification process: A case study in Hoa Binh, Vietnam. Environ Earth Sci. 2016;75(5):430.
21- Ildoromi A, Safari Shad M. Land use change prediction using a hybrid (CA-Markov) model. Ecopersia. 2017;5(1):1631-40.
22- Mushore TD, Mutanga O, Odindi J, DubeT. Assessing the potential of integrated landsat 8 thermal bands, with the traditional reflective bands and derived vegetation indices in classifying urban landscapes. Geocarto Int. 2017;32(8):886-99.
23- Sinha S, Sharma LK, Nathawat MS. Improved land-use/land-cover classification of semi-arid deciduous forest landscape using thermal remote sensing. Egypt J Remote Sens Sp Sci. 2015;18(2):217-33.
24- Sun L, Schulz K . The improvement of land cover classification by thermal remote sensing. Remote Sens. 2015;7(7):8368-90.
25- Barrett B, Nitze I, Green S, Cawkwell F. Assessment of multi-temporal, multi-sensor radar and ancillary spatial data for grasslands monitoring in Ireland using machine learning approaches. Remote Sens Environ. 2014;152:109-24.
26- Pencue-Fierro EL, Solano-Correa YT, Corrales-Muñoz JC, Figueroa-Casas A. A semi-supervised hybrid approach for multitemporal multi-region multisensor landsat data classification. IEEE J Sel Top Appl Earth Obs Remote Sens. 2016;9(12):5424-35.
27- Mohammady M, Amiri M, Dastorani J. Modeling land use changes of Ramin city in the Golestan province. J Spat Plan. 2016;19(4):141-58.
28- Wulder MA, White JC, Loveland TR, Woodcock CE, Belward AS, Cohen WB, et al. The global landsat archive: Status, consolidation, and direction. Remote Sens Environ. 2016;185:271-83.
29- Lu D, Weng Q. A survey of image classification methods and techniques for improving classification performance. Int J Remote Sens. 2007;28(5):823-70.
30- Madhura M, Venkatachala S. Comparison of supervised classification methods on remote sensed satellite data: An application in Chennai, South India. Int J Sci Res. 2015;4(2):1407-11.
31- Castillo M, Muñoz-Salinas E. Controls on peak discharge at the lower course of Ameca River (Puerto Vallarta graben, west-central Mexico) and its relation to flooding. CATENA. 2017;151:191-201.
32- Jia K, Wei X, Gu X, Yao Y, Xie X, Li B. Land cover classification using landsat 8 operational land imager data in Beijing, China. Geocarto Int. 2014;29(8):941-51.
33- Namdar M, Adamowski J, Saadat H, Sharifi F, Khiri A. land-use and land-cover classification in semi-arid regions using independent component analysis (ICA) and expert classification. Int J Remote Sens. 2014;35(24):8057-73.
34- Chuvieco E. Fundamentals of satellite remote sensing. Boca Raton: CRC Press; 2009.
35- Zoungrana BJ, Conrad C, Amekudzi LK, Thiel M, Da ED, Forkuor G, et al. Multi-temporal landsat images and ancillary data for land use/cover change (LULCC) detection in the Southwest of Burkina Faso, West Africa. Remote Sens. 2015;7(9):12076-102.
36- Sesnie SE, Hagell SE, Otterstrom SM, Chambers CL, Dickson BG. SRTM-DEM and landsat ETM+ data for mapping tropical dry forest cover and biodiversity assessment in Nicaragua. Rev Geogr Acad. 2008;2(2):53-65.